JOURNAL OF GEOPHYSICAL RESEARCH, VOL. 103, NO. C9, PAGES 18,599–18,609, AUGUST 15, 1998

Age determination of mixed water masses using CFC and oxygen data

Johannes Karstensen
Institut für Meereskunde der Universität Hamburg, Hamburg, Germany

Matthias Tomczak
Flinders Institute for Atmospheric and Marine Sciences, The Flinders University of South Australia, Adelaide, Australia

Abstract. We present a new method based on a combination of optimum multiparameter analysis and CFC/oxygen mixing analysis to determine the ages of water masses in regions of mixing. It enables us to follow water mass movements in greater detail than with other methods, which give only the combined pseudoage of a water mass mixture. We define the age of a water mass as the time a water parcel needs to spread from its source region, where it received its individual tracer characteristics, to the point of observation. The age distribution allows us to determine pathways of water masses, which differ from simple advection trajectories because the age is determined by a combination of advective and diffusive processes. We apply the method to hydrographic data along World Ocean Circulation Experiment section I5 in the south east Indian Ocean. In the thermocline, Indian Central Water (ICW) and Subantarctic Mode Water (SAMW) meet and mix. These distinct water masses have different formation mechanisms but similar temperature/salinity characteristics. It is shown that the convective formation of SAMW is a major ventilation mechanism for the lower Indian thermocline. In the eastern part of the south Indian Ocean, SAMW dominates the oceanic thermocline and is found to be about 5 years old. Pure ICW is present only in the thermocline of the region 48°-55°E, with increasing age with depth, confirming the subduction theory. While most SAMW joins the equatorward gyre movement of the southeastern Indian Ocean, some of it propagates westward through turbulent diffusive mixing, reaching 55°E after 15-20 years. It takes ICW some 25-30 years to reach 110°E.

1. Introduction

The use of oceanic tracers offers an opportunity for following the pathways of water masses through the ocean and for quantifying their fractions as they mix [*Wüst*, 1935]. Tracer distributions are controlled by a combination of transport processes associated with the oceanic circulation and mixing and by reactive processes associated with the major biogeochemical cycles [*Chester*, 1990]. When tracing water mass pathways by analyzing water mass mixtures (i.e. in temperature/salinity (T/S) or temperature/oxygen (T/O_2) diagrams), the task is to extract the amount of different source water masses from the observed mixture and if necessary keep track of changes resulting from biogeochemical processes in a quantitative manner.

Paper number 98JC00889.
0148-0227/98/98JC-00889$09.00

On regional scales, when the analysis is restricted to an area of a few hundred kilometers, biogeochemical modification can be ignored, and even mixing situations involving a multitude of water masses can be analyzed quantitatively without consideration of aging processes [*Hinrichsen and Tomczak*, 1993]. On the basin scale the fate in space and time of individual water masses which do not mix to any large degree over long distances can be evaluated from transient tracers [*Jenkins*, 1987; *Doney and Bullister*, 1992; *Warner and Weiss*, 1992] as well as from oxygen, if the change of oxygen concentration with time, the oxygen utilization rate (OUR), is known [*Jenkins*, 1982, 1987].

The present work is concerned with situations where both mixing and aging are important contributors to the tracer distribution. Optimum multiparameter (OMP) analysis can be applied to such situations to resolve the mixing if an additional term is introduced to compensate changes in the nutrient and oxygen field due to biogeochemical cycling. To determine the true age of an individual water mass involved in the mixing

process from oxygen observations, we require an accurate knowledge of the OUR. We derive an estimate of the OUR from age information determined from CFC (F-11 and F-12) observations in unmixed waters, where only little internal mixing occurs.

CFCs have no natural sources in the ocean and are introduced from the atmosphere, where their concentration has increased since their commercial production began shortly after 1930 (Figure 1). In the ocean, CFCs are not affected by biogeochemical cycles, and their distribution is solely determined by advection, mixing, and diffusion. The oxygen distribution in the ocean, however, reflects advection, mixing, and diffusion as well as biogeochemical cycling activity. Comparison of the age information in CFC and oxygen fields (biogeochemical cycling activity calculated into an age via OUR) can therefore be used to determine the age of the water, that is, the time that has passed since the water mass formation. If more than one water mass is present, each water mass has its own age, and the aim of the analysis is to determine the individual age of each water mass separately. This places a minimum requirement on the available number of time dependent tracers. If two water masses dominate the situation, we have to derive two age fields, while two time dependent tracers are needed.

The analysis proceeds in two stages. As a first step, the linear mixing model of a modified OMP analysis [*Mackas et al.*, 1987; *Tomczak and Large*, 1989] is used to analyze the mixing conditions in the region. This leads to the determination of the water mass fractions contained in the mixture and of the source T/S properties (temperature and salinity of the water masses involved in the mixing process in their formation regions). In a second step these T/S source values are used to calculate initial oxygen and CFC surface uptake values for the whole atmospheric time history (for oxygen just one value), using the corresponding solubility functions [*Weiss*, 1970; *Warner and Weiss*, 1985] and 100% saturation of the tracers. This procedure is justified provided the water masses are formed in the surface mixed layer through air/sea interaction processes. OMP analysis then finds source water mass properties which correspond to surface mixed layer values. We then reformulate the mixing problem in terms of mixing equations for the tracer uptake of the ocean. The equations express tracer uptake as functions of the spreading times for each water mass, where the mixing fractions are known from OMP analysis. For each tracer the solution relates the observed tracer concentration to all possible combinations of water mass age and oceanic tracer uptake history. A unique solution, which fixes the ages of all participating water masses, is found by combining the information from a number of tracers (here: F-11, F-12, and oxygen). The minimum number of time dependent tracers which is necessary to find a unique age solution equals the number of water masses in the mixture.

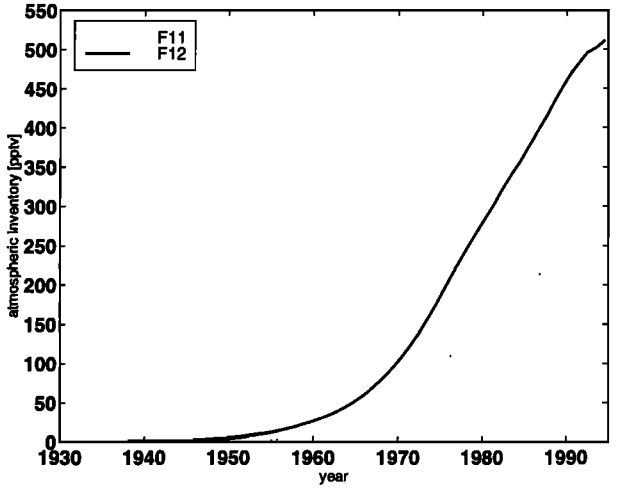

Figure 1. Time history of atmospheric F-11 and F-12 concentrations (S. Walker, P. Salameh, and R. Weiss, personal communication, 1995).

At present, the capacity of numerical models to follow water masses through the ocean and to evaluate their ages even under a state of very high dilution surpasses the capabilities of field oceanographers to derive corresponding quantities from their observations. Tracing the ages of individual water masses, as it is shown here, offers new possibilities for the evaluation of oceanic circulation and climate models and for detailed studies of ventilation processes. Our method offers opportunities to compare derived quantities from field observations with model results directly.

2. Method

The basis of our method is the assumption of linear mixing. This requires the dominance of turbulent mixing over other mixing processes in the ocean and allows the use of identical mixing coefficients for all parameters (temperature, salinity, oxygen, the nutrients, and the CFCs). The equations describing the parameter concentration C in a water parcel differ from parameter to parameter but can be grouped into three categories.

For a conservative parameter (i.e., temperature and salinity) the observed concentration $C_{\mathrm{obs}}^{\mathrm{cons}}$ is the result of an integration in time over all mixing events to which the parcel was exposed along its spreading path. If n water types contributed to these events, its mixing history can be expressed in a simple concentration equation in terms of the fractions x_i of the water types ($i = 1, 2, ..., n$) and their source concentrations C_i^{cons}:

$$C_{\mathrm{obs}}^{\mathrm{cons}} = \sum_{i=1}^{n} C_i^{\mathrm{cons}}\, x_i \qquad (1)$$

For a parameter with conservative mixing behavior but a time dependent source function (given by its atmospheric concentration history and transfer function), the observed concentration $C_{\mathrm{obs}}^{\mathrm{trans}}$ is the result of mixing be-

tween water masses with different oceanic tracer uptake $C_i^{\text{trans}}(t_i)$ depending on the year t_i of their formation:

$$C_{\text{obs}}^{\text{trans}} = \sum_{i=1}^{n} C_i^{\text{trans}}(t_i)\, x_i \qquad (2)$$

Finally, for a parameter which has a known source value in its region of origin (independent of time) but which participates in biogeochemical processes as it spreads through the ocean (i.e., oxygen and nutrients), the observed concentration $C_{\text{obs}}^{\text{noncons}}$ is the sum of two components:

$$C_{\text{obs}}^{\text{noncons}} = C^{\text{quasi-cons}} + C^{\text{bio/chem}} \qquad (3)$$

The first component $C^{\text{quasi-cons}}$ represents the development of the concentration field without inclusion of biogeochemical changes (i.e., as the result of oceanic mixing only). This component of the parameter can be identified with (1). Relating the second, the biogeochemical component $C^{\text{bio/chem}}$, to time (in the case of oxygen with the OUR) it can be identified with (2). Equation (1) forms the basis of the classical OMP analysis [*Tomczak and Large*, 1989], while (2) forms the basis for our age determination in a mixture of water masses. To achieve this, we rewrite (2) in terms of the time as the unknown variable. In the present case, mixing of two water masses containing the time dependent tracers CFC (F-11 and F-12) and oxygen (with a suitable OUR), the solution of (2) is a functional relationships between the ages of the two water masses: one derived from the a CFC component (either F-11 or F-12) and another one derived from oxygen. The solution is found by equating the relationships. Because the time history of oceanic CFC uptake is strongly nonlinear, equating the relationships is most easily done in graphical form by determining the intersection of two curves.

2.1. Stage 1: Optimum Multiparameter Analysis

OMP water mass analysis is now a standard tool in oceanography. It resolves observations of water mass mixtures into source water mass fractions by representing source water masses through source water types (SWT) [*Mackas et al.*, 1987; *Tomczak and Large*, 1989; *Maamaatuaiahutapu et al.*, 1992; *Hinrichsen and Tomczak*, 1993; *Klein and Tomczak*, 1994]. The SWT contributions x_i for each data point are obtained by finding the best linear mixing combination in the parameter space defined by temperature, salinity, oxygen, and nutrients which minimizes the residuals in a nonnegative least squares sense [*Lawson and Henson*, 1974]. The mass conservation ($\sum x_i = 1$) is an additional mixing constraint.

In the present application for the southern Indian Ocean thermocline the parameter fields are the result of mixing between two water masses with quasi-linear parameter relationships. OMP analysis represents them by a total of four source water types. We modified the classical OMP analysis [*Tomczak and Large*, 1989] by adding another column representing the biogeochemical transfer to the water type matrix:

$$\begin{array}{llcll} \sum_{i=1}^{4} T_i\, x_i & & = & T_{\text{obs}} & +R_T \\ \sum_{i=1}^{4} S_i\, x_i & & = & S_{\text{obs}} & +R_S \\ \sum_{i=1}^{4} \mathrm{O}_{2,i}\, x_i & -a\Delta\mathrm{O}_2 & = & \mathrm{O}_{2,\text{obs}} & +R_{\mathrm{O}_2} \\ \sum_{i=1}^{4} \mathrm{PO}_{4,i}\, x_i & +a\Delta\mathrm{PO}_4 & = & \mathrm{PO}_{4,\text{obs}} & +R_{\mathrm{PO}_4} \\ \sum_{i=1}^{4} \mathrm{NO}_{3,i}\, x_i & +a\Delta\mathrm{NO}_3 & = & \mathrm{NO}_{3,\text{obs}} & +R_{\mathrm{NO}_3} \\ \sum_{i=1}^{4} x_i & & = & 1 & +R_\Sigma \end{array} \qquad (4)$$

Here the observed values of temperature T_{obs}, salinity S_{obs}, oxygen $\mathrm{O}_{2,\text{obs}}$, phosphate $\mathrm{PO}_{4,\text{obs}}$, and nitrate $\mathrm{NO}_{3,\text{obs}}$ and their respective residuals R define the columns on the right-hand side. The values T_i, S_i, $\mathrm{O}_{2,i}$, $\mathrm{PO}_{4,i}$, and $\mathrm{NO}_{3,i}$ define the fixed parameter values of the four source water types. The new column on the left-hand side, $(-a\Delta\mathrm{O}_2{:}a\Delta\mathrm{PO}_4{:}a\Delta\mathrm{NO}_3)$, is an expression of the Redfield ratio [*Redfield et al.*, 1963] which links the change in oxygen concentration with the remineralization of nutrients. Adding this column to the system of equations takes care of the effect of changes in source water type definitions due to biogeochemical influences. The first two rows are the mixing equations for the two conservative parameters, temperature and salinity, the next three rows are the mixing equations for the nonconservative parameters, and the last row expresses the condition of mass conservation. The resulting system is formally similar to a subset of equations used by *Anderson and Sarmiento* [1994] in their determination of Redfield ratios for the world ocean. The solution procedure is different here, mainly because we used fixed source water types to calculate the fractions x_i.

For OMP analysis the mixing process in the present case is formally given by contributions from four source water types ($\mathrm{SWT}_{1\text{ to }4}$). All points on the line $\mathrm{SWT}_{1/2}$ as well as all points on the line $\mathrm{SWT}_{3/4}$ form a water mass (A and B). The final SWT contributions are found by a simultaneous solution in all parameter spaces [*Lawson and Henson*, 1974]. Figure 2 demonstrates how the extended OMP analysis proceeds in the case of two subspace combinations of conservative and nonconservative parameters. For two conservative parameters (left diagram), OMP analysis determines the contributions from all four SWT directly. These contributions can be recalculated into two source water types marked as solid circles on the parameter definition curves of A and B. The observational data (data_{obs}) is the result of mixing between water masses A and B along the dashed line. For a nonconservative parameter (right diagram) the observational data_{obs} are also affected by biogeochemical processes. Introducing the Redfield ratio in (4) separates these effects from the conservative mixing solution, replacing the observational data_{obs} by the corrected values data_{org}. In our application we used the Redfield ratios derived by *Anderson and Sarmiento* [1994] as 170:1:16 for $-a\Delta\mathrm{O}_2{:}a\Delta\mathrm{PO}_4{:}a\Delta\mathrm{NO}_3$.

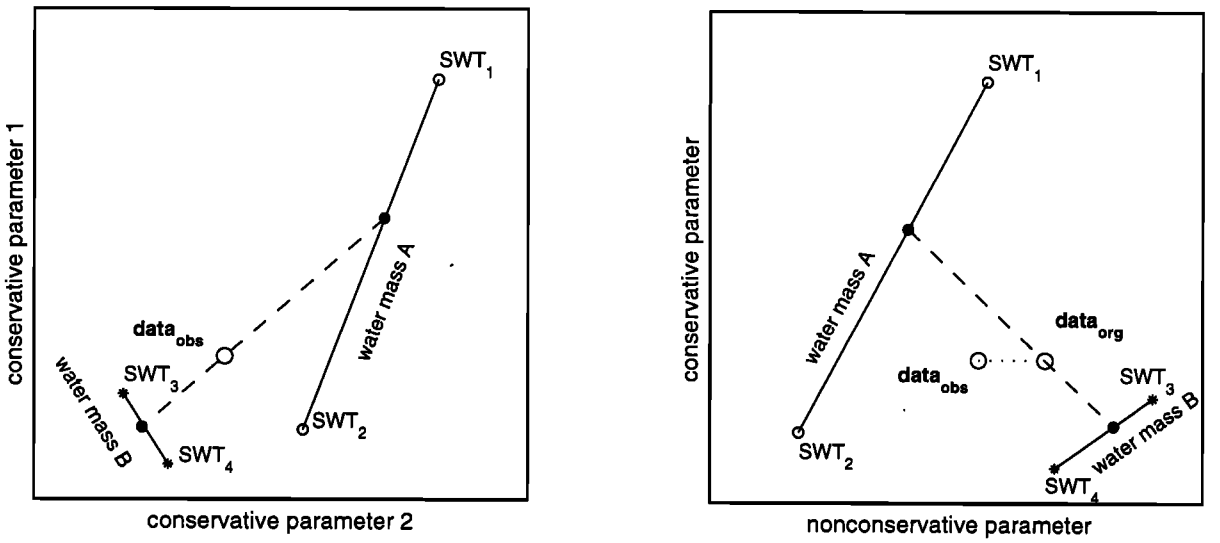

Figure 2. A sketch of mixing in the oceanic thermocline displayed in different parameter subspaces: (left) in a parameter subspace of two conservative parameters and (right) in a parameter subspace defined by one conservative and one nonconservative parameter (see text for details).

All water mass definition curves are derived in the same way by plotting the parameter against temperature in the formation region, assuming that the water mass was formed recently. In practice, the definition curves are derived from hydrographic casts in the formation region representing temperature/parameter relationships. Although some water parcels found at depth are still located in the formation region, they have already acquired a certain residence time, and a linear regression of oxygen versus temperature includes the effect of aging. Here we call the source oxygen values derived from the T/O_2 diagram the "local" source values of oxygen concentration. "Local" source values can be used for OMP analysis if one is only interested in the water type contributions and not in their age. Our CFC/oxygen age model discussed below determines true age, the time since the parcel left the mixed layer, and therefore requires "initial" oxygen values, that is, the oxygen concentration acquired by the water mass during active contact with the atmosphere. These can be derived from the oxygen solubility equation [*Weiss*, 1970] with the aid of the calculated T/S source values as described below.

2.2. Stage 2: Time Dependent Tracer Equations for CFC and Oxygen

OMP analysis gives the water mass fractions x_i encountered at all observation points. To derive individual ages for the two water masses, we rewrite the tracer equation (2), using the temperatures T_i^{source} and salinities S_i^{source} of the source water types and their fractions x_i and introducing the sea water solubility [*Weiss*, 1970; *Warner and Weiss*, 1995] and atmospheric concentration history (Figure 1) of the tracers:

$$\mathrm{CFC}_{\text{obs}} = \sum_{i=1}^{n} \mathrm{CFC}_{i,\text{atmos}}(t_i)\ \mathrm{solub}(T_i^{\text{source}}, S_i^{\text{source}})\ x_i \tag{5}$$

Here $\mathrm{CFC}_{\text{obs}}$ is the observed tracer concentration, $\mathrm{solub}(T_i^{\text{source}}, S_i^{\text{source}})$ is the sea water solubility of F-11 and F-12, respectively, and $\mathrm{CFC}_{i,\text{atmos}}(t_i)$ is the atmospheric tracer concentration in the formation region of source water type i at the time t_i of its formation. In a situation where a water mass spreads without mixing, (5) can be solved for a single tracer. In general, n independent tracers are required if n water masses are involved. The situation of interest here shows the mixing of two water masses. It is thus possible to determine the individual ages on the basis of measurements of only two time dependent tracers.

If we identify $\mathrm{solub}(T_i^{\text{source}}, S_i^{\text{source}})$ in (5) with the solubility function of oxygen [*Weiss*, 1970] and $\mathrm{CFC}_{i,\text{atmos}}$ (t_i) with the atmospheric oxygen concentration (which does not change with time), we can determine the oxygen concentrations $O_{2,i}^{\text{quasi-cons}}$ which the source water types SWT_i had at their time of formation ($C^{\text{quasi-cons}}$ in (3)). In the absence of biogeochemical processes the sum of the products then gives the oxygen concentration of the water mass mixture at the data point. The difference between this oxygen value and the observed value represents the modification of the oxygen concentration through biogeochemical processes ($C^{\text{bio/chem}}$ in (3)). Under idealized conditions (uniform Redfield ratios in space and time, oxygen uptake at the

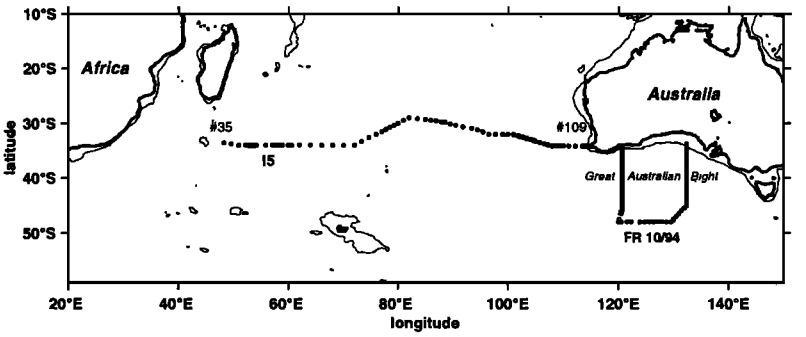

Figure 3. Cruise tracks and station positions for World Ocean Circulation Experiment (WOCE) section I5, stations 35 to 109, and for the WOCE expedition of *R/V Franklin* (FR10/94).

surface given by the oxygen saturation equation, 100% saturation at the surface and initial source water types) it equals the apparent oxygen utilization (AOU) as well as the value $a\Delta O_2$ in (4). This value can be related to water mass age through the oxygen utilization rate OUR [*Riley*, 1951; *Jenkins*, 1982, 1987]:

$$\text{OUR} = \frac{\text{unmixed AOU}}{\text{spreading time (age)}} \; [\mu\text{mol kg}^{-1}\text{y}^{-1}] \quad (6)$$

In the real ocean the change of oxygen content is the result of various processes. Water in the surface layer of the ocean is mostly oversaturated ($\sim$ 5%) because of the presence of air bubbles introduced by wave action [*Broecker and Peng*, 1982]. The biogeochemical processes affecting the oxygen concentration vary because of photosynthesis and associated chemical reactions in the euphotic zone and oxidation of detritus and bacterial activity in the deeper layers of the water column. We assume here that the water parcels participate in surface layer processes for a relatively short time only. Most of their time they spend spreading and mixing below the mixed layer and euphotic zone, and the assumption of a well-defined OUR is justified. It is also worth noting that the OUR determined from transient tracer data represents an integral quantity [*Thiele and Sarmiento*, 1990], which reduces its uncertainty. Under these conditions, (2) can be rewritten with (6) to

$$O_2^{\text{bio/chem}} = \sum_{i=1}^{n} \text{OUR}\; t_i \; x_i \quad (7)$$

We derived the OUR for the southern Indian Ocean from observations of CFC and oxygen obtained in regions of pure water masses, where no significant internal mixing has occurred. Here the difference between CFC content and oxygen concentration is due to the time de-

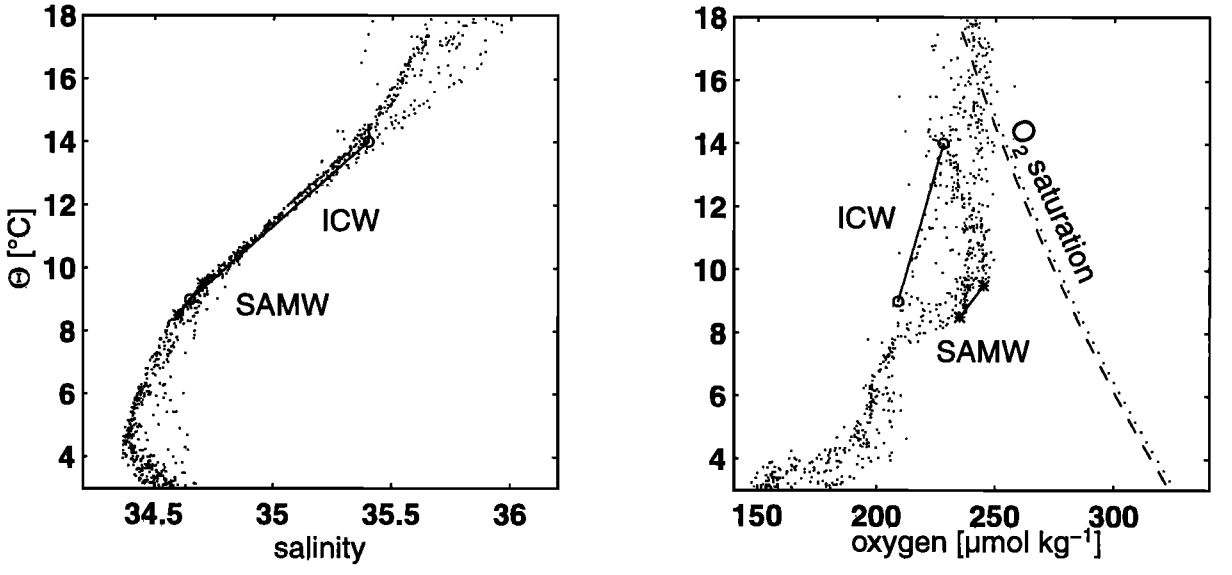

Figure 4. (left) Temperature-salinity and (right) temperature-oxygen relationships for bottle data from station 35 to 109 of WOCE section I5. The lines indicate the "local" water mass definitions for Indian Central Water (ICW) (open circles) and Subantarctic Mode Water (SAMW) (asterisks). The temperature-oxygen diagram also includes the oxygen saturation values for salinities S =34 (dashed line) and S =35 (dotted line).

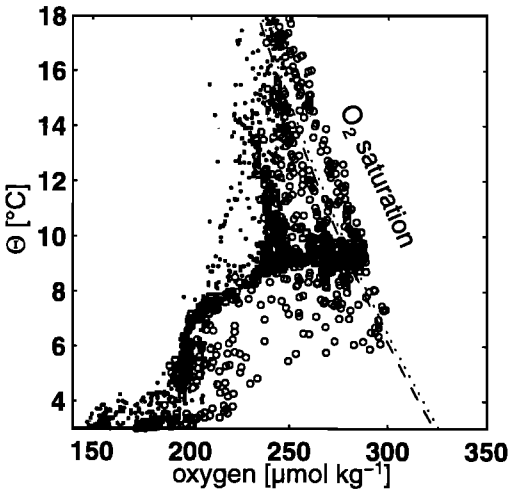

Figure 5. Temperature-oxygen diagram for all bottle data from FR10/94 (open circles) and WOCE section I5 (solid circles). Oxygen saturation values are shown for salinities S =34 (broken line) and S =35 (dotted line). Data points to the right of these lines indicate oversaturation in the surface layer. The SAMW signal is seen as a cluster of high oxygen points in the temperature range 8.5°-9.5°C.

pendent input of CFC at the surface (age indicator) and to the modification of the oxygen concentration from biological and chemical factors thereafter (AOU). We verified the assumption on little mixing with the aid of a simple one-dimensional advection/diffusion model representing the larger-scale spreading of a single water mass with internal mixing only.

3. Data

The region covered by the present application of our method is the southern Indian Ocean at 32°S from about 48°E to the Australian coast (Figure 3). These data were collected during the World Ocean Circulation Experiment (WOCE) on WOCE section I5. Data from three shorter sections (*R/V Franklin* FR10/94) along 120°E from the Australian coast to 48°S, then along 48°S eastward to 132°E, and along 132°E to the Australian coast (Figure 3) were used only to define Subantarctic Mode Water (SAMW) source water types for the present application. A detailed description of section I5 is given by *Toole and Warren* [1993] and *Fine* [1993]. *Schodlok et al.* [1997] give a detailed description of the sections in the Great Australian Bight.

In the temperature range 9°-14°C the data display the well-known linear T/S (Figure 4, left) and T/O_2 relationship (Figure 4, right) of Indian Central Water (ICW) [*You and Tomczak*, 1993]. ICW is formed by subduction in the subtropical region of negative wind stress curl as a result of Ekman pumping [*Montgomery*, 1938; *Luyten et al.*, 1983]. In addition, the data contain a strong signal of high oxygen at the lower level of the thermocline, identified by *Fine* [1993] as Subantarctic Mode Water (SAMW). SAMW is produced by deep convective overturning north of the Antarctic Circumpolar Current [*McCartney*, 1977]. The same water mass was found in the Great Australian Bight (Figure 5), where its significantly higher oxygen content indicates its proximity to the convection region [*Ribbe and Tomczak*, 1997]. The difference in the T/O_2 relationships of ICW and SAMW is an indication of these different formation mechanisms.

4. Results

Table 1 shows the "local" and "initial" (in parentheses) water type definitions for the permanent thermocline in the southern Indian Ocean. We derived these in the usual manner by plotting all parameter relationships for WOCE section I5 and FR10/94 and identifying the envelopes of all points as source water masses (see Figure 4). The situation in the southern Indian Ocean is of particular interest because SAMW is in the source parameters concentration nearly identical to ICW but has a particular formation region (covered by the FR10/94 data). Most of its properties overlap entirely with those of ICW, while the main discriminator in parameter space is oxygen. In the region under investigation it is much higher in SAMW than in ICW, indicating more recent formation caused by the different formation mechanism (convective overturning) [*Mc-*

Table 1. "Local" and "Initial" Definition of Water Masses for OMP Analysis

	ICW		SAMW		
	Lower SWT	Upper SWT	Lower SWT	Upper SWT	Weights
temperature °C	9.0 (9.0)	14.0 (14.0)	8.5 (8.5)	9.5 (9.5)	0.5
salinity	34.65 (34.65)	35.4 (35.4)	34.6 (34.6)	34.7 (34.7)	0.5
O_2 µmol kg^{-1}	209.0 (281.6)	228.0 (251.9)	235.0 (284.9)	245.0 (278.4)	2
PO_4 µmol kg^{-1}	1.47 (1.0)	0.6 (0.32)	1.4 (1.2)	1.16 (0.98)	2
NO_3 µmol kg^{-1}	20.0 (13.5)	7.0 (2.0)	20.0 (16.8)	16.0 (14.0)	2

Values in the parentheses are initial definition values. Abbreviations are as follows: OMP, optimum multiparameter; SWT, source water type; ICW, Indian Central Water; and SAMW, Subantarctic Mode Water

Cartney, 1977]. Determining the weights for the various parameters (following the usual procedure as described by *Tomczak and Large* [1989]), this leads to the unusual situation that the highest weight does not go to temperature or salinity but to oxygen and nutrients (Table 1).

4.1. Water Mass Distribution on WOCE Section I5

Figure 6 shows the resulting ICW water mass content (percentage) for the analyzed data on WOCE I5 section. As expected [*Sprintall and Tomczak*, 1993], ICW dominates the western part of the section. SAMW is seen to intrude from the east at the source density range [*Fine*, 1993]. West of 48°E, OMP analysis produces very large residual errors, indicating the presence of other water masses which are transported southward along the African coast. We therefore limited our investigation to the region east of 48°E.

The parameters required for the age determination are derived from regions of nearly "pure" water masses, which we define as all stations with a water mass content >95% of either ICW or SAMW. Stations with nearly pure ICW are found west of 55°E and in the upper thermocline farther east (Figure 6). A core of nearly pure SAMW is found at the density level σ_Θ = 26.8-26.9 kg m^{-3} between 90°E and 114°E. In both regions the oxygen concentration is not significantly influenced by mixing, and the departure from oxygen saturation is mainly the result of biogeochemical processes. Temperature and salinity, however, are unchanged from the values obtained during water mass formation. This allows us to determine the amount of oxygen consumed between water mass formation and the time of our observations and to define the initial oxygen concentration for the ICW source water types with the solubility function [*Weiss*, 1970]. Initial phosphate and nitrate (Table 1) are then calculated with the Redfield ratio [*Anderson and Sarmiento*, 1994].

4.2. Age of Pure ICW and SAMW

Before we proceed to determine the ages of ICW and SAMW in the mixing region, we have to calculate the age of the pure water masses and to calculate the oxygen utilization rate (OUR). The age within pure water masses can be derived directly from the CFC observations by comparing the observed CFC (F-11 and F-12) value with the atmospheric time history of CFC. The procedure is based on the assumption that the effect of mixing within a water mass [*Warner and Weiss*, 1992] is negligible. To test this assumption, we applied the atmospheric CFC time history input (Figure 1) to a simple one- dimensional advection/diffusion model with fixed solubility (for T=12°C and S=35) as a boundary condition:

$$\frac{dC}{dt} = k\frac{\partial^2 C}{\partial^2 x} - u\frac{\partial C}{\partial x}$$

Here C is the concentration of a tracer, t is time, k is the horizontal eddy diffusion, and u is the downstream advection velocity along the spreading surface in x direction. The model simulates the spreading of a single pure water mass along an isopycnal horizon, with no mixing of external water masses. Given the increase of atmospheric CFC with time (positive input gradient), any internal mixing such as eddy diffusion should lead to a decrease in the CFC concentration and therefore to a change in age prediction to older ages. The equation was solved with an implicit Crank-Nicolson finite differences method [*Crank and Nicolson*, 1947] with full-slip boundary condition, forward in time and centered in space. The differencing method is stable for the chosen grid and time space. We used a time interval Δt of 1 month, grid space of Δx =100 km, advection velocity u =0.01 m s^{-1}, and horizontal eddy diffusion k =1800 m^{2}s^{-1} [*Warner and Weiss*, 1992]. The initial condition was zero concentration on all points in the 3000 km domain. The integration was done for the period of 1931 to 1990. With the constant advection velocity, the model gives us an "advection only" age$_{\text{pure}} = \frac{\text{distance}}{c}$ (as it is assumed in our pure water mass age prediction) which can be compared with the age analyzed in the same way as in the case of pure water on I5 from the model output data. Figure 7 shows the F-11 relative age prediction error (F-12 looks similar but is not shown here) for all modeled observation years. The error is mainly influenced by the sign and strength of the gradient in the CFC time history. A change in

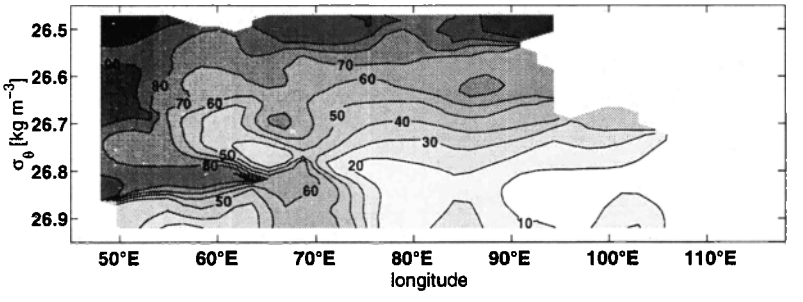

Figure 6. ICW water mass content (percentage) along WOCE section I5 derived from local water type definitions. SAMW water mass content is given by 100 - ICW (percentage).

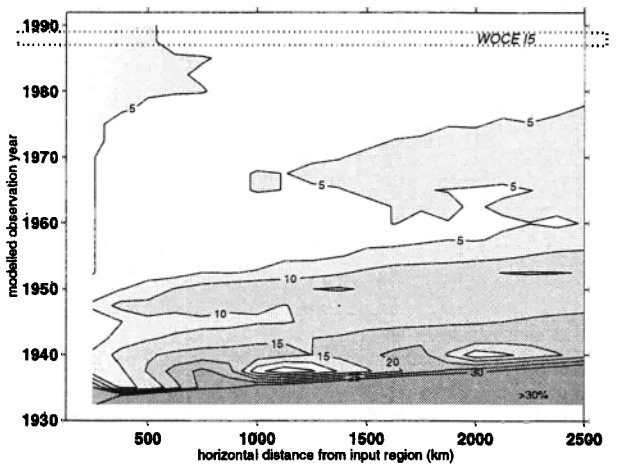

Figure 7. Relative age error (percentage) as a function of horizontal distance from the input region, obtained from modeled F-11 data. The WOCE I5 data observation period is marked.

sign of the gradient (as at the beginning of the 1980s) can compensate the effect of eddy diffusion on the tracer field, even in simulations with k values of 5000 m^2s^{-1} (not shown here). At the observation time (marked as WOCE I5 in Figure 7) the relative error is generally less then 10%, confirming our assumption about the negligible effect of internal mixing. It is therefore valid to relate the observed apparent oxygen utilization (AOU) with the age from the I5 CFC data to obtain the oxygen utilization rate (OUR) along the spreading path of the pure water masses (Figure 8). The OUR is remarkably constant in both water mass cores at about $5\mu mol\,kg^{-1}y^{-1}$ for densities $\sigma_\Theta > 26.6$ kg m^{-3} and in good agreement with the log linear best fit to ^{3}He data for the north Atlantic Subtropical gyre [*Jenkins*, 1982]. Using an optimization algorithm (Nelder-Mean simplex algorithm), we derive the best fit for the density range $27.0 > \sigma_\Theta > 26.4$ kg m^{-3} as

$$\begin{aligned} \mathrm{OUR} &= 97.8\exp(-5.8(\sigma_\Theta - 26)) \\ &+ 3.6\exp(-0.0041(\sigma_\Theta - 26))\ [\mu mol\ kg^{-1}y^{-1}] \end{aligned}$$

The scatter increases toward lower densities (Figure 8), that is, toward the surface. This is the region where water parcels left the biologically active surface layer only recently. They have been exposed to the various biogeochemical processes for a relatively short time only and thus have a highly variable OUR. Differences in the input gradient of F-11 and F-12 in the 1980s may cause a shifts in the F-11 ages toward more older ones compared to F-12 through internal mixing. This result in a systematic smaller OUR deduced from F-11 toward the surface.

To test the consistency of the pure water age prediction in the presence of measurement errors, we generated 100 new data values for each data point by adding random noise to F-11, F-12, oxygen data, and the OUR (± 0.9 mean standard deviation). Figure 9 shows the relative error in age prediction by comparing the mean of F-11 and F-12 derived ages to the mean of the ages derived by oxygen with the aid of the OUR. The resulting errors at densities $\sigma_\Theta > 26.6$ kg m^{-3} are generally less than 30%. The increase of the relative age error toward the surface reflects mainly the misfit of the OUR from different F-11 and F-12 ages toward the surface (see Figure 8).

4.3. Ages of Mixed Water Components

Having established the necessary parameters, we now proceed to the determination of ICW and SAMW ages in the mixing region. The analysis is based on the assumption of the density dependent OUR, 100% saturation of CFCs and oxygen in the source region, and constant Redfield ratios [*Anderson and Sarmiento*, 1994]. In the regions of pure water masses (>95% ICW and >95% SAMW) the amount of oxygen consumed since formation in the mixed layer ($a\Delta O_2$ in (4)) was used to obtain water mass age through (7). In the region of mixed water masses the same quantity $(a\Delta O_2)/\mathrm{OUR}$ represents a "mixed age" a quantity which is not easy to interpret. However, using the OUR calculated above and the water mass fractions x_i determined from OMP analysis, we write (7) as a linear relation of the individual water mass ages t_1 and t_2 of the ICW and SAMW components in the mixture

$$\frac{a\Delta O_2}{\mathrm{OUR}} = t_1x_1 + t_2x_2 \qquad (7')$$

A second relationship is required to find the absolute water mass ages t_1 and t_2. We obtain this informa-

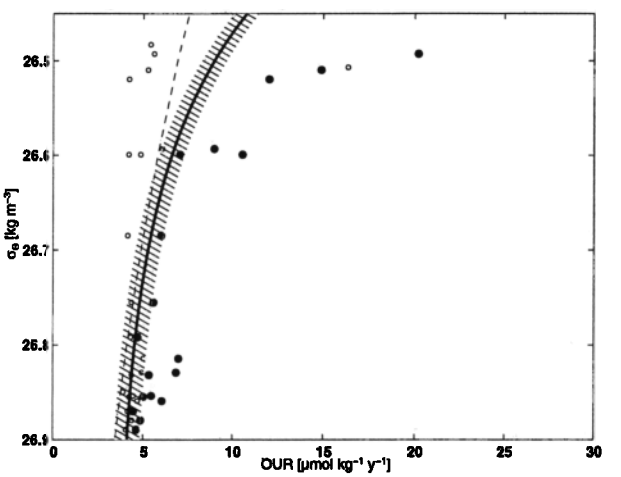

Figure 8. Oxygen utilization rate (OUR) in "pure" ICW and SAMW as a function of density. Values obtained from F-12 (solid circles) and F-11 (open circles). The dashed line shows the log linear fit of *Jenkins* [1982] derived from ^{3}He data in the Sargasso Sea; the dashed line is the best fit from a Nelder-Mean simplex optimization to I5 data. The hatched area indicates the mean standard deviation of our fit.

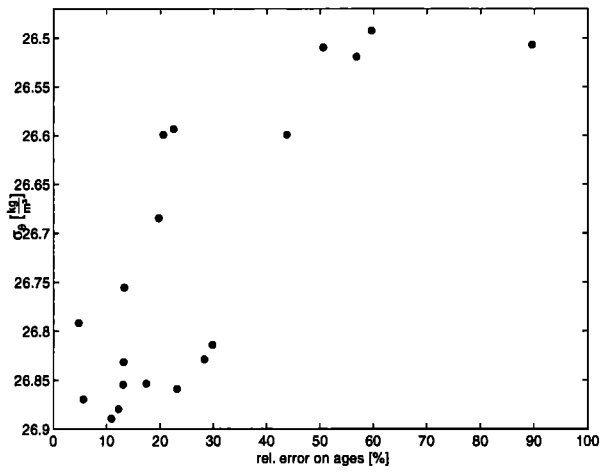

Figure 9. Relative age error in pure water, indicating the sensitivity of the predicted ages on measurement errors (F-11, F-12, oxygen, and OUR).

tion from the CFC measurements. At each data point the observed CFC concentration CFC_{obs} can be written with (5) as

$$\begin{aligned} CFC_{obs} &= CFC_1(t_1)\ \text{solub}(T_1^{source}, S_1^{source})\ x_1 \\ &+ CFC_2(t_2)\ \text{solub}(T_2^{source}, S_2^{source})\ x_2 \end{aligned} \quad (5')$$

where subscript 1 refers to ICW, say, and subscript 2 refers to SAMW. $CFC_i(t_i)$ is the CFC (F-11 or F-12) concentrations in pure ICW and SAMW, respectively,

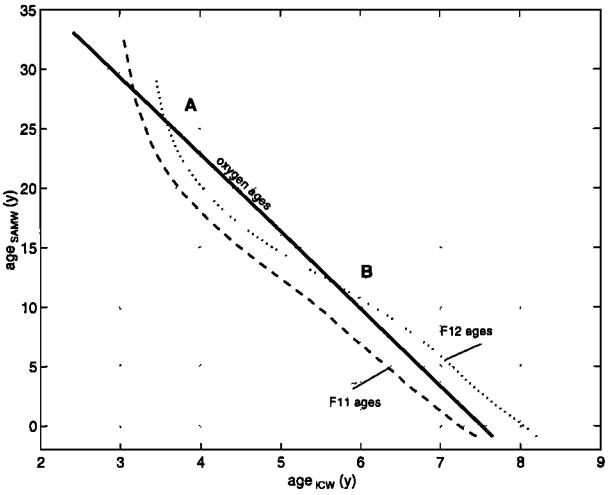

Figure 10. The relationships between age of the SAMW component (t_2 of equations (6) and (7)) and the age of the ICW component (t_1 of equations (6) and (7)) in the mixing region. The bold straight line is calculated from equation (6); the dashed and dotted lines are calculated from equation (7) as applied to F-11 and F-12, respectively. The age of the ICW component in the mixture is found to be 3.5 years from F-12 and 3.1 years from F-11; the age of the SAMW component is 28.1 and 25.4 years, respectively. The analyzed age is the mean (3.3 years for ICW and 26.75 years for SAMW).

at the (unknown) times t_i. The times are determined by looking for all corresponding time pairs (t_1 and t_2) of the atmospheric input history (Figure 1, transferred with source T/S values and the solubility function) resulting in the observed CFC value. Equations (5') and (7') give two relationships between t_1 and t_2. We can use them to produce a graph of t_2 against t_1 (Figure 10). The intersection point of two curves (one from oxygen and one from a CFC component) gives us the absolute ages of ICW and SAMW in the mixed regime. Having three time dependent tracers available, we find the final age by building the mean of O_2/F-11 and O_2/F-12 age pairs intersections (A in Figure 10). Point B in Figure 10 is interpreted as being not valid, because of the missing F-11 intersection. Table 2 summarizes this for a one specific data point as an example. To test the robustness of the result, we produced 100 different OUR values for each data point by adding random noise with an amplitude of 0.9 (the mean standard deviation). Likewise, for all F-11 and F-12 values we produced 50 new data points by adding noise with an amplitude of the measurement standard deviation as given by *Fine* [1993]. The final age at each observation is the mean value of the analyzed data points (50 of O_2/F-11 and 50 of O_2/F-12). In the case of mixing with CFC free water (dilution of the CFC) the oxygen age pair will not intersect with the CFC ages, and a solution cannot be obtained.

4.4. Ages on WOCE Section I5

The age distribution of SAMW and ICW in the southeastern Indian Ocean derived from the present method was already reported as part of a special volume on the WOCE Indian Ocean survey [*Karstensen and Tomczak*, 1997]. In the context of the present paper, which focuses on a detailed description of the method, it is sufficient to summarize the main findings.

In the density range under consideration ($26.50 < \sigma_\Theta < 26.95$ kg m^{-3}), ICW dominates the water column in the west. Over 90% of SAMW content is found east of

Table 2. Measured and Calculated Values for Station 44 at 33°58.3'S, 57°02.1'E and 500.7 m Depth

Parameter	$Data_{obs}$	OMP Results	
		SAMW	ICW
Temperature °C	12.358	9.4	12.7
Salinity	35.135	34.69	35.14
O_2 μmol kg^{-1}	225.9		
F-11 pmol kg^{-1}	2.0651		
F-12 pmol kg^{-1}	1.0570		
fraction (%)		13	87
CFC/O_2 analysis		SAMW	ICW
F-11/O_2 age (years)		25.4	3.1
F-12/O_2 age (years)		28.1	3.5
Mean age (years)		26.75	3.3

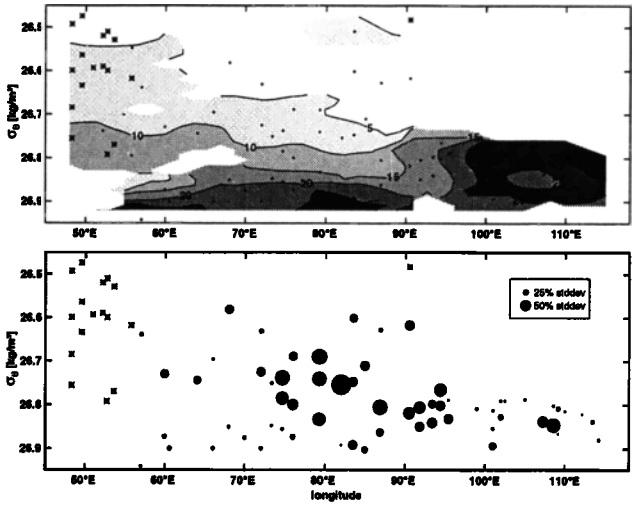

Figure 11. (top) Age (years) and (bottom) relative standard deviation of the ICW component in the water column along WOCE section I5. Asterisks indicate the region of ICW> 95%.

90°E at densities larger than $\sigma_\Theta = 26.80$ kg m^{-3}. The region of mixed water stretches from $\sigma_\Theta = 26.70$ kg m^{-3} near 90°E westward to 70°E, where it sinks rapidly to $\sigma_\Theta = 26.85$ kg m^{-3} and continues westward at that level. Figures 11 and 12 show the age distribution for ICW (Figure 11) and SAMW (Figure 12). To the west of 55°E, ICW is seen with an age of 4 to 6 years at densities less than $\sigma_\Theta = 26.65$ kg m^{-3} showing that the water is not recently formed but traveled some distance since leaving the surface without mixing with other water masses. ICW age increases with depth in agreement with the idea of formation trough subduction, which implies longer travel distances from the formation region for water found deeper in the water column. ICW age also increases eastward in agreement with the notion of eastward mean movement with the South Indian Ocean Current [*Stramma*, 1992]. The youngest SAMW is seen with an age of 4 to 7 years east of 110°E. This is closest to the formation region, which has been identified near 44°S at that longitude [*Ribbe and Tomczak*, 1997]. SAMW age increases westward, spreading against the mean circulation [*Karstensen and Tomczak*, 1997].

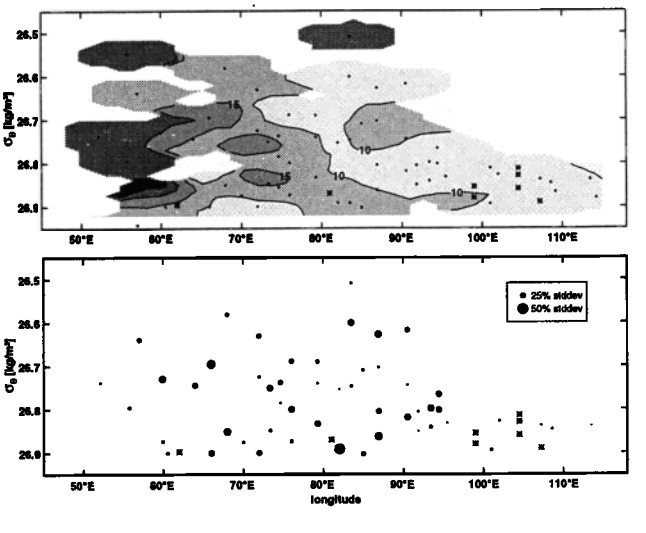

Figure 12. (top) Age (years) and (bottom) relative standard deviation of the SAMW component in the water column along WOCE section I5. Asterisks indicate the region of SAMW> 95%.

In summary, we have shown that true water mass age of thermocline water masses can be derived from observations of temperature, salinity, oxygen, nutrients, and CFCs. It is important to stress that the age determination is absolute, that is, calibrated in years, and that it can be performed in situations where the observations represent mixtures of water masses. This allows us to trace water masses well beyond their region of formation and quantify their mean spreading velocity [*Karstensen and Tomczak*, 1997].

Acknowledgments. We appreciate the critical and detailed comments from D.R. Quadfasel and two anonymous reviewers. This work was supported by grants of the Bundesminister für Bildung, Wissenschaft, Forschung und Technologie (03F0157A/WOCE IV) and of the Australian Research Council.

References

Anderson, L.A., and J.L. Sarimento, Redfield ratios of remineralization determined by nutrient data analysis, *Global Biogeochem. Cycles, 8,* 65-80, 1994.

Broecker, W.S., and T.-H. Peng, *Tracers in the Sea*, 690 pp., Lamont-Doherty Geol. Obs., Palisades, N. Y., 1982.

Chester, R., *Marine Geochemistry*, 698 pp., Chapman and Hall, New York, 1990.

Crank, J., and P. Nicolson, A practical method for numerical integration of partial differential equations of the heat-conduction type, *Proc. Cambridge Philos. Soc., 43,* 50-67, 1947.

Doney, S.C., and J.L. Bullister, A chlorofluorocarbonsection in the eastern North Atlantic, *Deep Sea Res., 39,* No. 11-12, 1857-1883, 1992.

Fine, R.A., Circulation of Antarctic Intermediate Water in the south Indian Ocean, *Deep Sea Res., Part I, 40,* 2021-2042, 1993.

Hinrichsen, H.H., and M. Tomczak, Optimum Multiparameter Analysis of the water mass structure in the western North Atlantic Ocean, *J. Geophys. Res., 98,* 10155-10169, 1993.

Jenkins, W.J., On the climate of a subtropical gyre: Decadal timescale variations in water mass renewal in the Sargasso Sea, *J. Mar. Res., 40,* Suppl., 265-290, 1982.

Jenkins, W.J., ^{3}H and ^{3}He in the Beta Triangle: Observations of gyre ventilation and oxygen utilization rates, *J. Phys. Oceanogr., 17,* 763-783, 1987.

Karstensen, J., and M. Tomczak, Ventilation processes and water mass ages in thermocline of the southeast Indian Ocean, *Geophys. Res. Lett., 24,* 2777-2780, 1997.

Klein, B., and M. Tomczak, Identification of diapycnal mixing through optimum multiparameter analysis, 2: Evidence for unidirectional diapycnal mixing in the front between North and South Atlantic Central Water, *J. Geophys. Res., 99,* 25275-25280, 1994.

Lawson, C.L., and R.J. Hanson, *Solving Least Square Problems*, 340 pp., Prentice-Hall, Englewood Cliffs, N. Y., 1974.

Luyten, J., J. Pedlosky, and H. Stommel, The ventilated thermocline, *J. Phys. Oceanogr., 13*, 292-309, 1983.

Mackas, D.L., K.L. Denman, and A.F. Bennett, Least squares multiple tracer analysis of water mass composition, *J. Geophys. Res., 92*, 2907-2918, 1987.

Maamaatuaiahutapu, K., V.C. Garcon, C. Provost, M. Boulhadid, and A.P. Osiroff, Brazil Malvinas Confluence: Water mass composition, *J. Geophys. Res., 97*, 9493-9505, 1992.

McCartney, M.S., Subantartctic Mode Water, in A voyage of discovery, *Deep Sea Res., 24*, Suppl., 103-119, 1977.

Montgomery, R.B., Circulation in the upper layer of the southern North Atlantic deduced with use of isentropic analysis, *Pap. Phys. Oceanogr. and Meteor., 6*, 1-73, 1938.

Redfield, A.C., B.H. Ketchum, and F.A. Richards, The influence of organism on the composition of sea water, in *The Sea*, vol. 2, edited by M.N. Hill, Wiley-Interscience, New York, pp. 26-77, 1963.

Ribbe, J., and M. Tomczak, On convection and the formation of Subantarctic Mode Water in the Fine Resolution Antarctic Model (FRAM), *J. Mar. Syst., 13*, 137-154, 1997.

Riley, G.A., Oxygen, phosphate and nitrate in the Atlantic Ocean, *Bull. Bingham Oceanogr. Collect., 31*, 1-126, 1951.

Schodlok, M.P., M. Tomczak, and N. White, Deep sections through the South Australian Basin and across the Australian-Antarctic Discordance, *Geophys. Res. Lett., 24*, 2785-2788, 1997.

Sprintall, J., and M. Tomczak, On the formation of Central Water and thermocline ventilation in the southern hemisphere, *Deep Sea Res., Part I, 40*, 827-848, 1993.

Stramma L., The South Indian Ocean Current, *J. Phys. Oceanogr., 22*, 412-430, 1992.

Thiele, G., and J.L. Sarmiento, Tracer dating and ocean ventilation, *J. Geophys. Res., 95*, 9377-9391, 1990.

Tomczak, M., and D.G.B Large, Optimum multiparameter analysis of mixing in the thermocline of the eastern Indian Ocean, *J. Geophys. Res., 94*, 16141-16149, 1989.

Toole, J.M., and B.A. Warren, A hydrographic section across the subtropical South Indian Ocean, *Deep Sea Res., Part I, 40*, 1973-2019, 1993.

Warner, M.J., and R.F. Weiss, Solubilities of chorofluorocarbons 11 and 12 in water and seawater, *Deep Sea Res., Part A, 32*, 1485-1497, 1985.

Warner, M.J., and R.F. Weiss, Chorofluoromethanes in South Atlantic Antarctic Intermediate Water, *Deep Sea Res., Part A, 39*, 2053-2075, 1992.

Weiss, R.F., The solubility of nitrogen, oxygen and argon in water and seawater, *Deep Sea Res., Oceanogr. Abstr., 17*, 721-735, 1970.

Wüst, G., Die Stratosphäre des Atlantischen Ozeans, in *Wissenschaftliche Ergebnisse der Deutschen Atlantischen Expedition auf dem Forschungs- und Vermessungsschiff Meteor 1925-27*, Vol. 6, pp. 109-288, A. Defant, Berlin, 1935.

You, Y., and M. Tomczak, Thermocline circulation and ventilation in the Indian Ocean derived from water mass analysis, *Deep Sea Res., Part I, 40*, 13-56, 1993.

J. Karstensen, Institut für Meereskunde der Universität Hamburg, Troplowitzstr. 7, 22529 Hamburg, Germany. (e-mail: karstens@ifm.uni-hamburg.de)

M. Tomczak, Flinders Institute for Atmospheric and Marine Sciences, The Flinders University of South Australia, GPO Box 2100, Adelaide, South Australia 5001, Australia. (e-mail: matthias.tomczak@flinders.edu.au)

(Received March 11, 1997; revised November 6, 1997; accepted February 12, 1998.)